SYNTHESIS AND CHARACTERIZATION OF GOLD NANOPARTICLES FOR NON-INVASIVE CANCER TREATMENT

CHIN GUO FENG

MASTER OF ENGINEERING SCIENCE

LEE KONG CHIAN FACULTY OF ENGINEERING AND SCIENCE
UNIVERSITI TUNKU ABDUL RAHMAN
APRIL 2018

ABSTRACT

SYNTHESIS AND CHARACTERIZATION OF GOLD NANOPARTICLES FOR NON-INVASIVE CANCER TREATMENT

Chin Guo Feng

This research is dedicated to develop an alternative cancer treatment method by utilizing nanotechnology. As the removal of the tumours located in the vital organ, or the poorly accessible tissues is highly precarious, alternative cancer treatment is an urge for those cancers remained irremediable. While the neoangiogenesis produces leaky blood vessels around the tumour, colloidal particles take this advantage of size in passively targeting to the cancerous cells. The gold nanoparticles, also known as nanogold, have been received wide interests in the research applications in medicine, biopharmaceutical and chemical industries over the past decade. The bioinertity nature of the nanogold has brought multiple possibilities to its utilization in the alternative cancer treatment. This research has successfully produced two types of gold nanoparticles, namely the spherical gold nanoparticles, or gold nanosphere, and rod shape gold nanoparticles, or gold nanorod. The gold nanosphere recorded the size at 30.58 nm ± 0.72 nm, while the gold nanorod recorded an average aspect ratio of 2.98 ± 0.16, which fall within the targeted size range of 20 nm to 50 nm. Physical characterizations of the synthesized gold nanoparticles are reported.

DECLARATION

I hereby declare that the dissertation is based on my original work except for quotations and citations which have been duly acknowledged. I also declare that it has not been previously or concurrently submitted for any other degree at UTAR or other institutions.

Name : CHIN GUO FENG

Date : _____

APPROVAL SHEET

This dissertation/thesis entitled "**SYNTHESIS AND CHARACTERIZATION OF GOLD NANOPARTICLES FOR NON-INVASIVE CANCER TREATMENT"** was prepared by CHIN GUO FENG and submitted as partial fulfillment of the requirements for the degree of Master of Engineering Science at Universiti Tunku Abdul Rahman.

Approved by:

_____

(Dr. LEE POH FOONG)
Date: ……..
Assistant Professor/Supervisor
Department of Mechatronics and BioMedical Engineering
Faculty of Engineering and Science
Universiti Tunku Abdul Rahman

_____

(Dr. TANG PEK YEE)
Date: ……..
Assistant Professor/Co-supervisor
Department of Mechatronics and BioMedical Engineering
Faculty of Engineering and Science
Universiti Tunku Abdul Rahman

LIST OF TABLES

LIST OF FIGURES

LIST OF ABBREVIATIONS

AgNPs	Silver nanoparticles
AuNPs	Gold nanoparticles
BSA	Bovine serum albumin
CTAB	Hexadecyltrimethyl-ammonium bromide
DDS	Drug delivery system
DI	Deionized
DNA	Deoxyribonucleic acid
EF-TEM	Energy filtered transmission electron microscope
EPR	Enhanced permeability retention
FE-SEM	Field emission scanning electron microscope
GNR	Gold nanorod
GNS	Gold nanosphere
LSPR	Localized surface plasmon resonance
NIR	Near infra-red
nm	Nanometer
NP	Nanoparticles
RNA	Ribonucleic acid
PEG	Poly ethylene glycol
PPTT	Plasmonic photothermal therapy
SPR	Surface plasmon resonance
UV	Ultra-violet
Vis	Visible

TABLE OF CONTENTS

CHAPTER ONE

INTRODUCTION

1.1 Background

The number of cancer patients over the globe has increased dramatically during the past few decades. While the surgical excision of tumours is a highly effective method in cancer treatment, the tumours located in the vital organ or the poorly accessible tissues remained as a challenge for us to remove it. Hence, finding alternative ways to cure cancers is an urge for those who are still remain "incurable" now, for the sake of human mankind.

For this, the introduction of nanotechnology has provided multiple opportunities and possibilities to the cancer treatments, as well as modern science-based medicine studies. The use of nanotechnology in medicine, also known as nanomedicine (Esther et al., 2015), is expected to change the conventional impression to the cancer diagnosis, detection, and most importantly, the cancer treatment methods. Thanks to nanomedicine, ultra-fine particles that are much smaller than human body cells, typically in nano size scale, can penetrate through the protein channels of the cell membrane (Zhao et al., 2016). With this, the possibilities for the nanoparticles to interact with the cells, particularly cancer cells are infinite. The nanoparticles can serve as the

drug delivery vehicle (Guo et al., 2016) that bring the targeted drug into the cell, which significantly increasing the efficacy of the treatment.

Also, nanoparticles that possesses special electrical and optical properties are capable to perform the physical treatment to targeted human body part or tissue. The example of the treatment method in this context is the plasmonic photothermal therapy (PPTT) (Bhana et al., 2016, Afifi, 2013, Huang and El-Sayed, 2011). On the other hand, various types of materials are being synthesized into nanoparticles. However, the noble metal nanoparticles (Rai et al., 2015) had been studied the most for the past decades due to their ease in synthesis, surface modification and their size and shape distribution. In particular, gold nanoparticles (Granmayeh Rad et al., 2011) have exhibited excellent characteristics in the size and shape distribution, together with various synthesis methods that are established to synthesize the gold nanoparticles. The unique characteristic of the gold nanoparticles, such as the surface plasmon resonance (SPR), (Baik, 2011, El-Sayed, 2005, Kihm, 2012) which can be tuned into the desired spectrum range by alternating the shape of the gold nanoparticles, has enable the gold nanoparticles to establish various possibilities and capabilities in the cancer treatments.

Lastly, gold metal is well-known with its excellent biocompatibility (Naahidi et al., 2012, Arsianti, 2011). With this, gold nanoparticles are expected biocompatible to biological system and human body. This is rather important to prevent the systemic cytotoxicity in the *in-vivo* injection of the gold nanoparticles.

1.2 Aims and Objectives

The aim of this study is to carry out a strategy in synthesizing and characterizing the gold nanoparticles. Objectives of this research are outlined as well.

- To synthesize gold nanoparticles in the range of 20 nm – 50 nm.

  This targeted size range fits to the leaky vasculature as tumour blood vessels formed during neoangiogenesis are lack of the tight junctions and the gaps can be ranged from 100 nm – 200 nm (Ribatti et al., 2007). Also, the tumour vasculature has greater vascular compared to normal subcutaneous vasculature (Narang and Varia, 2011).

- To synthesize gold nanoparticles in the spherical and rod shape.

  The gold nanoparticles are synthesized into two different shapes to study the surface plasmon resonance effect.

- To characterize the synthesized gold nanoparticles in size, stability with PEG 1000, and the surface plasmon resonance.

CHAPTER TWO

LITERATURE REVIEW

2.1 Cancer Nanotechnology: Definition and Application

The studies of cancer nanotechnology have become the focus of discussion for the alternative cancer treatment methods over the past decades. Particles that is smaller than 100 nm, particularly in the size range of 20 nm – 50 nm, known as nanoparticles, has become a useful and powerful branch of the research field to the studies of nanotechnology. The dimensions of nanoparticles in this size range is similar to the biomolecules, for instance: the diameter of human DNA double helix is about 2 nm (Inaga et al., 1991), proteins that are range from 1 nm to 20 nm , and the cell membrane range from 6 nm to 10 nm. This has led to the application of the nanotechnology in medical science, which is also known as nanomedicine (Esther et al., 2015, Etheridge, 2012, DeMesster and Barlow, 1988). As for cancer nanotechnology (Kawasaki and Player, 2005), it is the branch of nanomedicine that characterizes the interaction of nanoscale systems with cellular and molecular components specifically related to cancer diagnosis, as well as its therapy.

2.1.1 Importance of Nanotechnology in Cancer Treatment

The application of nanomedicine has gained much more attentions in biomedical applications due to the breakthroughs in nanotechnology (Chin et al., 2012). The incorporation of nanotechnology into the alternatives cancer treatment methods other than conventional cancer treatment methods has gained much attention over the past decades, especially in the case when the tumour located in the vital organs or the poorly accessible body tissues, or when the disease is beyond the cure ability of the conventional methods (Chin et al., 2013). With this, cancer nanotechnology is the key of possibilities that leads to useful research tools, advanced drug delivery systems, and new ways to diagnose and treat cancer disease or repair damaged tissues and cells (Jr, 2005).

2.2 Noble Metal and Their Nanoparticles

The noble metal is characterized as a metal group that is inert to chemical activity with the atmosphere, moistures and even mild acids (Rai et al., 2015, Jain, 2010). They are the several metallic chemical elements that have extraordinary resistance to oxidation and corrosion even at high temperatures. In the periodic table, the grouping of noble metal is not clearly defined. The examples of noble metal include rhenium, ruthenium, rhodium, palladium, silver, osmium, iridium, platinum, and gold. Besides, noble metals do not develop rust or undergo corrosion due to their lack of reactivity. Therefore, most of the noble metals are consider as stable, and have a long-life span.

With the excellent stability and long life span characteristics, many noble metals are being synthesized into nanoparticles, such as platinum (Zhou et al., 2012), silver (Vlăsceanu et al., 2016, Bernard et al., 2014, Vaidyanathan et al., 2009) and gold (Papasani, 2012, DeMesster and Barlow, 1988, Ghosh et al., 2008). Noble metal nanoparticles had attracted a significant interest from the researchers and scientists around the world owing to their unique physical properties , ease in synthesis, surface modification, and their size and shape distribution (Akbarzadeh, 2009). The applications of noble metal nanoparticles are being investigated and studied intensively due to their difference of physical properties when in the bulk state compared to their nanoscale. The difference of physical properties, particularly the optical property might be due to the quantum size effect resulting in the specific electronic and optical properties. By manipulating the size and shape of the nanoparticles, their optical properties can be tuned to the targeted range (Kihm et al., 2012). Besides, noble metal nanoparticles are well known for their strong interactions with light through the resonant excitations of the collective oscillations of the conduction electrons on the particles, which is known as surface plasmon resonances (SPR) (Lombardi et al., 2010, Granmayeh Rad et al., 2011).

With this, novel application possibilities of noble metal nanoparticles in the cancer treatments are to be discovered by the researchers and scientist, opening further opportunities to replace the conventional cancer treatment methods.

2.3 Gold Nanoparticles

The usage of gold in medical applications has a long history. It is not only been used in both Eastern and Western traditional medicine (Cho, 2009), while the modern medicine has used the gold-containing medicine in the treatment for many diseases (Aillon, 2009). In nature, gold is an inert noble metal which does not chemically react to any compound. The earliest medical use of gold can be traced back to the Chinese in 2500 BC (Huaizhi and Yuantao, 2000), where red colloidal gold is used as the, "drug of longevity" for the emperor . Besides, the Indian's Ayurvedic medicine is still using red colloidal gold for the rejuvenation and revitalization during old age (Mukherjee et al., 2013, Kumar et al., 2016). As for the Western medicine, colloidal gold was commonly used to deal with alcoholism since the nineteenth century (Richards et al., 2002), and it is still being used in the applications of the controls of dependency on alcohol, nicotine, caffeine, and carbohydrates (Mukherjee et al., 2013). Since 1927, gold has been used in the treatment of rheumatoid arthritis (Richards et al., 2002), epilepsy and syphilis (Daniel and Astruc, 2004).

Today, the application of AuNPs in nanomedicine has gained much more attention in recent years. The applications include targeted drug delivery system (DDS), gene and protein delivery, biological imaging and in implants (e.g. pacemaker and stents) (Aillon, 2009). Also, many studies have suggested that AuNPs are bioinert and can be used safely (Richards et al., 2002, Ghosh et al., 2008, F. K. Alanazi, 2010).

2.4 Silver Nanoparticles

The AgNPs is well known in medicine for antibacterial (Sheehy et al., 2014), antifungal (Flower et al., 2016), anti-viral (Palaniappan et al., 2015), and anti-inflammatory therapy (Hamouda, 2012). It has been well accepted and shown great success as a biocide against microbial infections (Flower et al., 2016), burns and diabetic skin ulcers. The study of AgNPs in cancer therapy and targeted drug delivery is being explore for the past decades. The AgNPs can be synthesized through an array of methods like spark discharging (Chen and Schluesener, 2008), electrochemical reduction (Tao et al., 2015, Jose et al., 2016), solution irradiation (Liu et al., 2017) and cryochemical synthesis (Sergeev et al., 1999). It exhibits a unique peak in the range of 400–460 nm and their synthesis is quantified based on the absorbance value obtained at the peak value (Chen and Schluesener, 2008). The biological activity of silver has been attributed to the presence of the Ag^{+} ion. Two examples of medicinal silver based compounds being used clinically are silver sulfadiazine (Sandri et al., 2013, Miller et al., 2012) and actisorb silver (Furr et al., 1994, Karonidis et al., 2011).

The anti-microbial activity of silver stems from the positively charged ion actively binding with negatively charged proteins, RNA and DNA to inhibit cell replication (Bhattacharyya et al., 2011). AgNPs (1–10 nm) bind to HIV-1 and drastically inhibited the HIV infection (Elechiguerra et al., 2005, Lara et al.,

2011) compare to a bovine serum albumin (BSA) surface modified silver particle (Galdiero et al., 2011). Many attempts have been made to use AgNPs as an anti-cancer agent. However, the targeting of AgNPs towards cancer cells involves certain limitations, for instance the toxicity of AgNPs towards the body cells (Faedmaleki et al., 2014). Also, although the targeting of cancer cells using AgNPs has proven to be effective, but neither the exact mechanism of action nor the modes of activation of the downstream signalling molecules have been revealed yet (Vaidyanathan et al., 2009).

2.5 Gold Nanoparticles in Cancer Theranostic

2.5.1 Introduction of Gold Nanoparticles in Cancer Treatment

As discussed in the earlier section, AuNPs have been suggested as bioinert and can be used safely in the human medical treatment (Naahidi et al., 2012). This section will discuss the types of the AuNPs, and the physical and optical properties of the AuNPs that can be utilized in the cancer treatment.

2.5.2 Types of Gold Nanoparticles

There are several types of AuNPs, namely spherical AuNPs, or gold nanosphere (GNS), rod-shaped AuNPs, or gold nanorod (GNR) and other shapes of the AuNPs.

2.5.2.1 Gold Nanosphere

Spherical AuNPs, or the gold nanosphere (GNS) is the most native shape of the synthesized AuNPs (Chin et al., 2013). GNS displays a single strong absorption band that is not present in the spectrum of a solid layer of deposited gold on substrate. The synthesis of gold nanosphere starts with the nucleation, where the initial period of nucleation favoured the formation of gold aggregates, resulting from the reduction of Au(III) by citrate, which deposit on the gold nuclei to produce small monodisperse gold nanosphere.

2.5.2.2 Gold Nanorod

As for gold nanorod (GNR), which is the AuNPs in cylindrical or rod shape, is the secondary development of the AuNPs (Dickerson et al., 2008, Murphy et al., 2011). In a GNR, two separate absorption bands are observed due to the transverse and longitudinal structures of the GNR. The presence of {110} facet in addition to the existing {111} and {100} facets in GNS, possessed a higher surface energy (Wang, 2000). This additional {110} facet makes the structural difference and is absent in GNS.

2.5.2.3 Others

Other than spherical and rod shape, there are many other shapes of AuNPs such as sub-octahedral, octahedral, decahedral, icosahedral multiple twined, multiple twined, irregular shape, tetrahedral, nanotriangles, nanoprisms, hexagonal platelets and many more. Each of these shapes of gold nanoparticle has its own unique characteristic and applications.

2.5.3. Physical and Optical Properties of Gold Nanoparticles

2.5.3.1 Localized Surface Plasmon Resonance

The surface plasmon resonance (SPR) is the collective oscillation of the electron cloud in certain material stimulated by incident light (Gormley et al., 2011). The resonance occurs when frequency of incident light photons matches the natural frequency of surface electrons oscillating against the restoring force of positive nuclei (Kihm et al., 2012). As for the SPR occurs in nanometer-sized structures, the term localized surface plasmon resonance (LSPR) is introduced.

In relation to this, AuNPs that possesses unique optical and electronic properties are well known for their strong interactions with light through the resonant excitations of the collective oscillations of the conduction electrons on the particles. The resonant frequency of the AuNPs is known to be dependent

on the size, shape, material properties and the surrounding medium of the AuNPs.

2.5.4 Plasmonic Photothermal Therapy

The application of plasmonic photothermal therapy (PPTT) uses the photon energy of the incident light source (Huang et al., 2008, Dickerson et al., 2008, Huang and El-Sayed, 2011), which is selectively administered into the targeted body part, and being converted into heat to provide a minimally-invasive oncological treatment by inducing the cellular hyperthermia. The advancement in the field of plasmonics has enabled new opportunities for the gold nanoparticles in its application. The photo-exciting conduction electrons which oscillate at the surfaces of the AuNPs produce local heat by non-radiative relaxation through electron–phonon and subsequent phonon–phonon coupling processes. The recently completed clinical trial NCT00848042 - Pilot Study of AuroLase (tm) Therapy in Refractory and/or Recurrent Tumors of the Head and Neck has utilized the principle of PPTT to study the efficacy of three different AuroShell groups.

CHAPTER THREE

METHODOLOGY

This chapter discusses the materials and chemicals, as well as the research methodology of this work.

3.1 Materials and Equipment

The project utilized the following chemicals: Gold chloride hydrate, trisodium citrate ($Na_3C_6H_5O_7$), L-ascorbic acid, hexadecyltrimethyl-ammonium bromide (CTAB), sodium borohydride ($NaBH_4$), poly ethylene glycol (PEG) (mw. 1000), and silver nitrate ($AgNO_3$). Deionized (DI) water (>18.2mΩ) was used throughout the study. Magnetic stirrer hotplate is used in the GNS synthesis process. The characterization of the synthesized AuNPs involved UV-Vis spectrophotometer, zetasizer, field emission scanning electron microscope (FE-SEM), and energy filtered transmission electron microscope (EF-TEM).

3.2 Synthesis Methods of Gold Nanoparticles

To synthesize the AuNPs, 10.0 mM Gold (III) ions stock solution was produced by dissolving 0.1 g of the gold chloride hydrate into 25.0 ml of deionized water. The stock solution was stored in dark and 4°C. When needed, 1.0 ml of the 10.0 mM gold (III) ions stock solution was diluted into 10.0 ml to make 1.0 mM gold (III) ions solution, and 20.0 ml to make 0.5 mM gold (III) ions solution. On the other hand, 4.0 mg of sodium borohydride ($NaBH_4$) was dissolved into 10.0 ml of deionized water to produce 0.01 M $NaBH_4$ solution. The solution was put in ice bath (0°C) and freshly prepared right before each experiment.

Similarly, 0.1 g of trisodium citrate ($Na_3C_6H_5O_7$) was dissolved in 10.0 ml of deionized water to produce 1% $Na_3C_6H_5O_7$ solution. The solution was also freshly prepared but in room temperature and right before each experiment. As for the poly ethylene glycol (PEG) solution, 0.33 g of PEG 1000 was dissolved in 10.0 ml of deionized water to produce 3.3% PEG solution. All glassware and instruments were cleaned by nitro-hydrochloric acid (3 parts of hydrochloric acid to 1 part of nitric acid), and rinsed by deionized water before use.

3.2.1 Gold Nanospheres

In this work, four samples of GNS were produced and investigated. They are 1) $NaBH_4$ reduced GNS solution with PEG 1000, 2) $NaBH_4$ reduced GNS solution without PEG 1000, 3) $Na_3C_6H_5O_7$ reduced GNS solution with PEG 1000, and 4) $Na_3C_6H_5O_7$ reduced GNS solution with PEG 1000. All samples were kept in room temperature without disturb after the synthesis. Stability test based on the changes of size and numbers of days were conducted on the four samples and the results were shown in the following sections.

3.2.1.1 Citrate-Reduction

The synthesis of GNS solution by citrate-reduction (Chin et al., 2013) was carried out by $Na_3C_6H_5O_7$ reduction under boiling temperature (100°C). 10.0 ml of 1.0 mM $HAuCl_4$ were heated on a hotplate with magnetic stirring. 0.5 ml of freshly prepared $Na_3C_6H_5O_7$ (room temperature) was added into the solution with continuous stirring and heating. The colour of the solution changed from lightly yellow to ruby red within five minutes and was removed from the hotplate while continuous stirring applied until the solution reaches the room temperature (Figure 3.1).

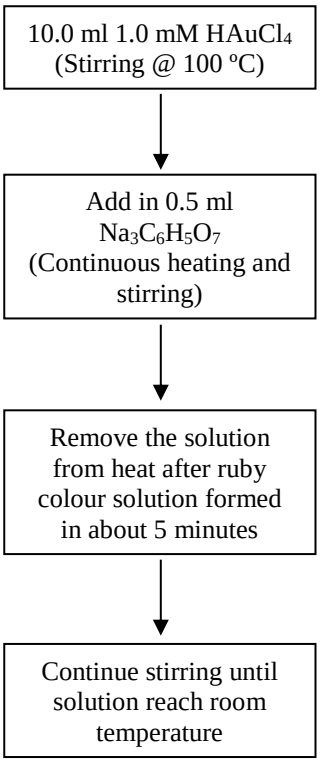

Figure 3.1. Flow chart of the synthesis of GNS solution by citrate-reduction.

3.2.1.2 Sodium Borohydride-Reduction

The synthesis of GNS solution by sodium borohydride-reduction (Papasani, 2012, DeMesster and Barlow, 1988, Ghosh et al., 2008) was conducted in room temperature. 10.0 ml of 1.0 mM $HAuCl_4$ was put in a conical flask and stirred vigorously on a magnetic stirrer. 0.5 ml of fresh prepared ice-cool (0°C) $NaBH_4$ was then added into the solution. The experiment took about 15 minutes and the colour of the solution slowly changed from light yellow to violet (Figure 3.2).

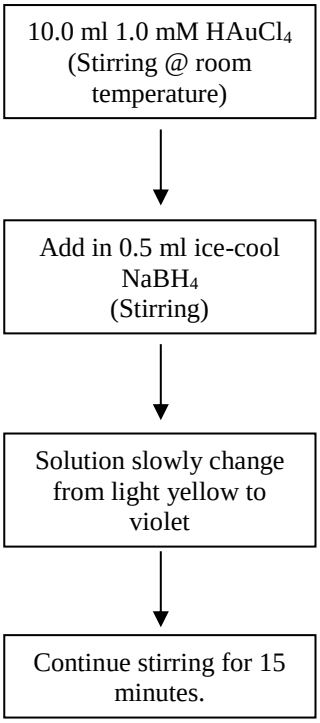

Figure 3.2. Flow chart of the synthesis of GNS solution by sodium borohydride-reduction.

3.2.2 Gold Nanorods

3.2.2.1 Seed-Mediated Growth

The synthesis of GNR was carried out by seed-mediated growth method (Murphy et al., 2011). A seed solution that contains ultrafine GNS seeds was first synthesized, and being added into the growth solution that contains free gold ions to allow the "growth" of GNR. The seed solution was prepared by the $NaBH_4$ reduction with the present of CTAB, where 5.0 ml of 0.2 M CTAB was mixed with 2.5 ml of 1.0 mM $HAuCl_4$ in a conical flask magnetic stirring,

followed by 600 µl of ice-cool $NaBH_4$ being slowly added into the solution to form a final brownish solution (Figure 3.3).

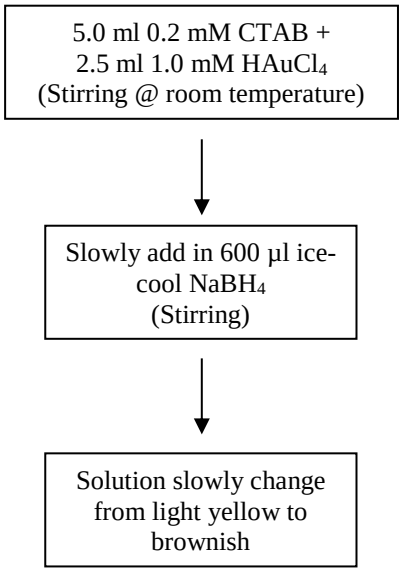

Figure 3.3. Flow chart of the synthesis of ultra-fine GNS seeds solution.

As for growth solution, 10.0 ml of 0.2 M CTAB and 10.0 ml of 1.0 mM $HAuCl_4$ together with 450 µl of 4.0 mM $AgNO_3$ were mixed in a conical flask with continuous stirring to form a yellowish solution, followed by adding 140 µl of 78.8 mM L-ascorbic acid into the solution. A colourless solution will be observed. Finally, 30 µl of the seed solution was added into the growth solution and gently mixed. The mixtures of the solutions were kept undisturbed under room temperature for 2 hours (Figure 3.4).

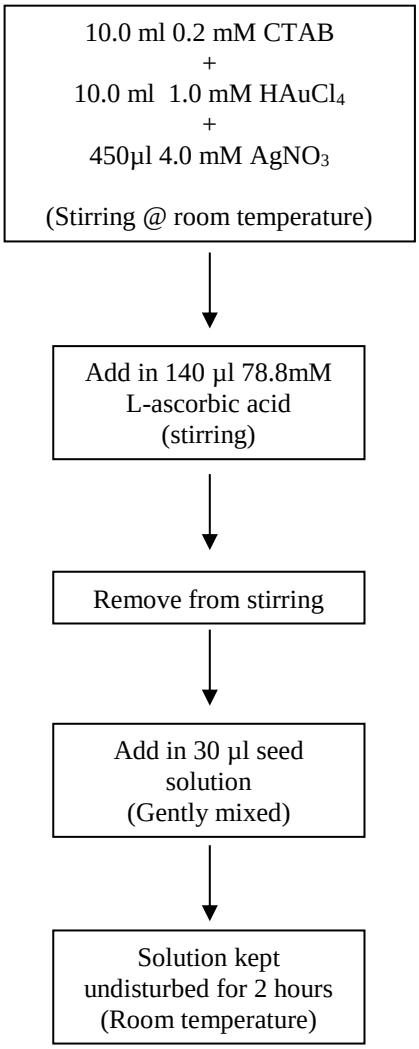

Figure 3.4. Flow chart of the synthesis of GNR solution

3.3 Characterization of Synthesized Gold Nanoparticles

The characterization of the AuNPs, namely size, shape and the localized surface plasmon resonance were done in this work. They are discussed in detail in this section.

3.3.1 Instrumentations

The UV-Vis spectrophotometer is used to characterize the LSPR of the synthesized gold nanoparticles. For the size, the zetasizer is utilized to obtain the hydrodymeter AuNPs. Besides, the research also utilized the FE-SEM and EF-TEM to enhance the characterization of the sizes and shapes of the synthesized AuNPs.

3.3.2 Sizes

The sizes of the synthesized AuNPs were determined by measuring the hydrodynamic diameter of the gold nanoparticles with the zetasizer. The instrument utilizes the mechanism of moving particles to measure the size of the particles via Stokes-Einstein equation (Flower, et al., 2016) as shown below.

$$d(H) = \frac{kT}{3\pi\eta D} \quad ,$$

where *d(H)* is the hydrodynamic diameter, *D* is the translational diffusion coefficient. *k* is the Boltzmann's constant (1.38064852 x 10^{-23} $m^2kgs^{-2}K^{-1}$), *T* is the absolute temperature (25°C) and η is the viscosity of the solution (0.8872). The emitted laser light of the zetasizer features a wavelength of 633 nm and the scattered information is detected upon a 173° angle via non-invasive backscattering systems detection (Figure 3.5). In this work, the hydrodynamic diameters for each of the gold nanoparticles solutions samples were measured

by using the zetasizer compatible disposable sizing cuvette for three times at 25°C. The results were averaged and expressed as mean Z-average.

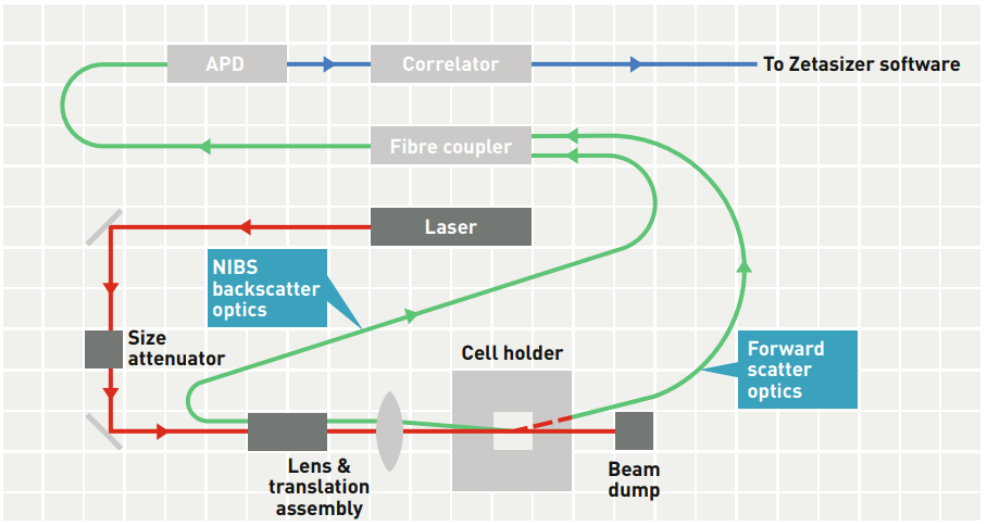

Figure 3.5. Block diagram of non-invasive back scattering systems of zetasizer.

3.3.3 UV-Vis Spectroscopy

An important property of the gold nanoparticles is that their LSPR can be detected by a UV-visible spectrometer. This enabled the researchers to characterize the GNS and GNR with UV-Vis spectroscopy. UV-Vis spectroscopy is the measurement of the incident light when it is passed through a sample which is based on the ability of the particles or molecules to absorb the ultraviolet and visible light from the light source. The absorption of light corresponds to the excitation of outer electrons in the molecule. The absorption can be measured at a single wavelength or on spectral extended range. The

absorption spectra of the samples were recorded by using UV-Vis spectrophotometer (Cary 50, Varian USA). The light is generated from the light source - a Xenon flash lamp and passed through the monochromator (Czerny-Turner) which splits the beam into different wavelengths out of the continuous spectrum (Figure 3.6). The intensity 'I_0' measured by the fraction of beam redirected using beam splitter. The transmitted intensity 'I' of the light beam is measured at the silicon diode photodetector and the absorbance (A) is calculated by the following formula under The Beer – Lambert Law (Flower, et al., 2016).

$$A = \log \frac{I_0}{i} \quad ,$$

The absorption is plotted as a function of the wavelength in an absorption spectrum.

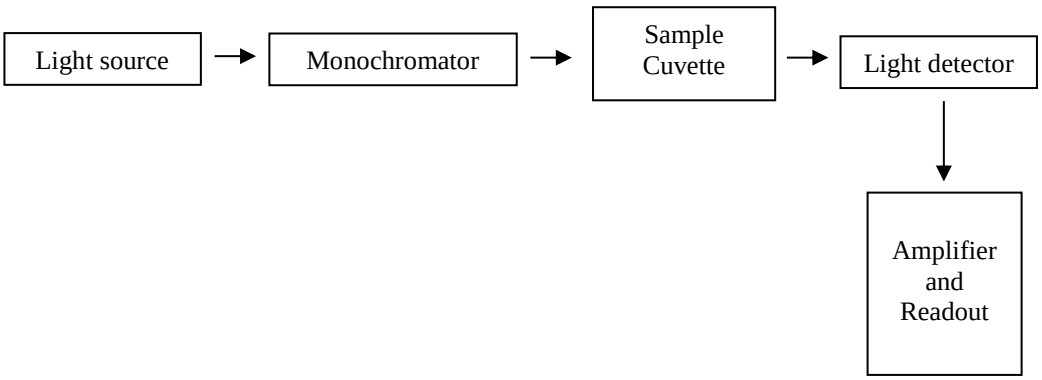

Figure 3.6. Block diagram of UV-Vis spectrometer.

3.3.4 Field Emission Scanning Electron Microscopy

Field emission scanning electron microscopy (FE-SEM) is a SEM based technique which employs a beam of highly energetic electrons to analyse materials on a very fine scale. The term “field emission” is adopted due to the emission of electrons from the surface of a conductor which is generated by a strong electric field. The microscopy images were taken in secondary electron imaging (SEI) mode, where the upper detector is used as the secondary electron detector. The selection of SEI mode is due to its better resolved images. The sample solution is dropped onto a carbon mounting tape prior to scanning under accelerating voltage of 3.0 kV and high vacuum mode.

3.3.5 Energy Filtered Transmission Electron Microscopy

The energy-filtered transmission electron microscopy (EF-TEM) utilizes the properties of the energy loss spectrum to increase contrast and remove the effects of chromatic aberration and create unique contrast effects in the image captured. The sample solution is dropped onto a 400 mesh copper grid held by a self-locking fine forceps. The solution is left on the copper grid for 1 minute, then the sample solution droplet is wicked to dryness using pieces of filter paper prior examination.

3.4 Stability Tests of Gold Nanoparticles

3.4.1 Stability Test for Gold Nanosphere

The stability of the GNS solution is measured by ability of the sample solution to maintain its size and uniformity over a certain period, e.g. four weeks in this study. In this work, the stability test was conducted by comparing the size and uniformity stability by the addition of the poly ethylene glycol (PEG) solution after the synthesis. The PEG with the molecular weight 1000 is used as the stabilizing agent. PEG 1000 is used in this study, instead of the PEG-Thiol (PEG-SH) to avoid the reaction between the stabilizing agent and the gold nanoparticles which might change the physical properties of the AuNPs. The test was conducted for both reducing agents used in the synthesis process, namely trisodium citrate and sodium borohydride. The sample solutions were tested by the zetasizer to obtain the size and the graph distribution.

3.4.1.1 Without PEG 1000 stabilizer

No PEG 1000 solution is added to the gold nanoparticles solution. To make the stability test relevant and valid, the synthesized gold nanoparticles solution was divided into 2 portions. Then, the solutions were kept in dark and under room temperature. Size and uniformity tests were done.

3.4.1.2 With PEG 1000 stabilizer

1.0ml of 3.3% PEG 1000 solution was added into the gold nanoparticles solution at the end of the reaction under room temperature. The samples were kept in dark and under room temperature. Size and uniformity tests were done.

CHAPTER FOUR

RESULTS AND DISCUSSION

4.1 Enhanced Permeability Retention Effect

There are many differences between the normal tissues as compared to the tumour tissues. Normal tissues have tight, continuous vessel walls, while the tumour tissues have discontinuous capillary walls and a large number of pores. With this, the AuNPs which possess Enhanced Permeability and Retention (EPR) effect has enabled the AuNPs to accumulate around the tumour tissues, but not in normal tissue (Ghosh et al., 2008). The accumulation of AuNPs around the tumour tissues is due to the leaky tumour blood vasculature in the tumour (Kolodgie et al., 2007). The leaky blood vasculature in the tumour forms during the neoangiogenesis, or tumour vascularisation with the limited oxygen and glucose diffusion capacity of the normal blood vessel around the tumour. This process occurs when the tumour size as small as several millimetres cube (Baban and Seymour, 1998). It enables the tumour cells to obtain sufficient oxygen and nutrients in order to proliferate and metastasize.

Besides, as the tumour enlarges very fast, tumour blood vessels formed during neoangiogenesis are often loosely bound with the gap in between the cells. This is because the tumour blood vessels formed during neoangiogenesis are lack of the tight junctions and the gaps can be range from 100 nm – 200 nm

(Ribatti et al., 2007). Also, the tumour vasculature has greater vascular compared to normal subcutaneous vasculature (Narang and Varia, 2011). The tumour tissues are lack of lymphatic system which functions to eliminate the lipophilic and polymeric materials from them. Hence, once the AuNPs entered into the tumour tissues, they cannot be eliminated easily (Ribatti et al., 2007). This phenomenon has provided a passive tumour targeting mechanism by accumulation of AuNPs in the tumour (Narang and Varia, 2011).

4.2 Characterization of the Gold Nanoparticles

This work has successfully synthesized the gold nanosphere and gold nanorod. The research methodology which enabled the synthesized of the size range of 20 nm – 50 nm spherical and rod shape particles with high uniformity were optimized. The gold nanoparticles were characterized using Zetasizer, FE-SEM, EF-TEM, and UV-Vis spectroscopy. The result of the synthesizing work, as well as the characterization of the synthesized AuNPs are discussed in this chapter.

4.2.1 Characterization of the Gold Nanosphere

4.2.1.1 Size Distribution by Intensity

The size distribution by intensity results of four GNS samples produced are listed in Figure 4.1 – Figure 4.4, and Table 4.1 recorded the peak values and the Z-average:

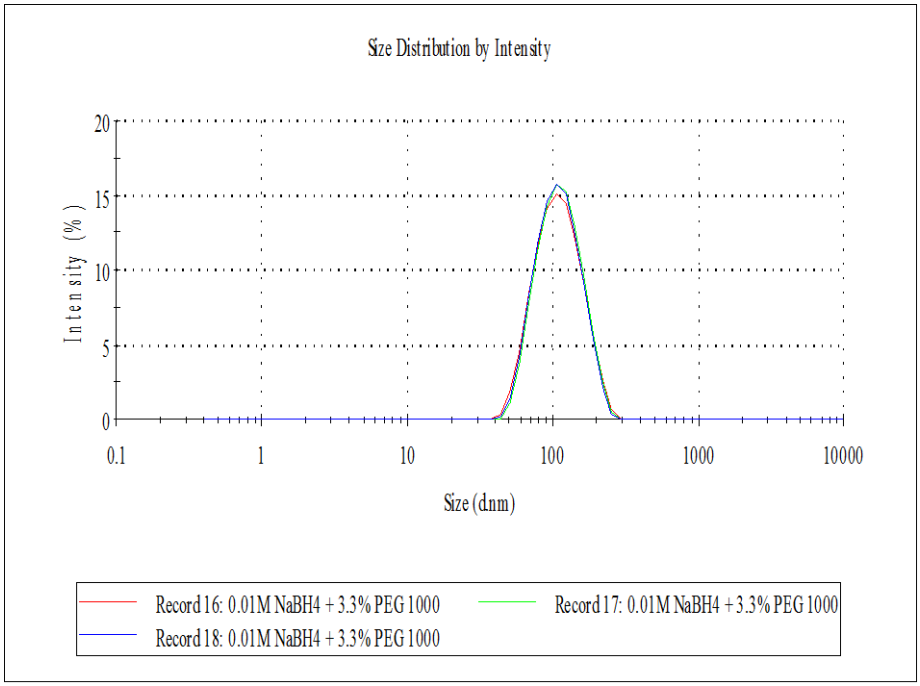

Figure 4.1 . Size distribution by intensity of GNS reduced by $NaBH_4$ with PEG 1000.

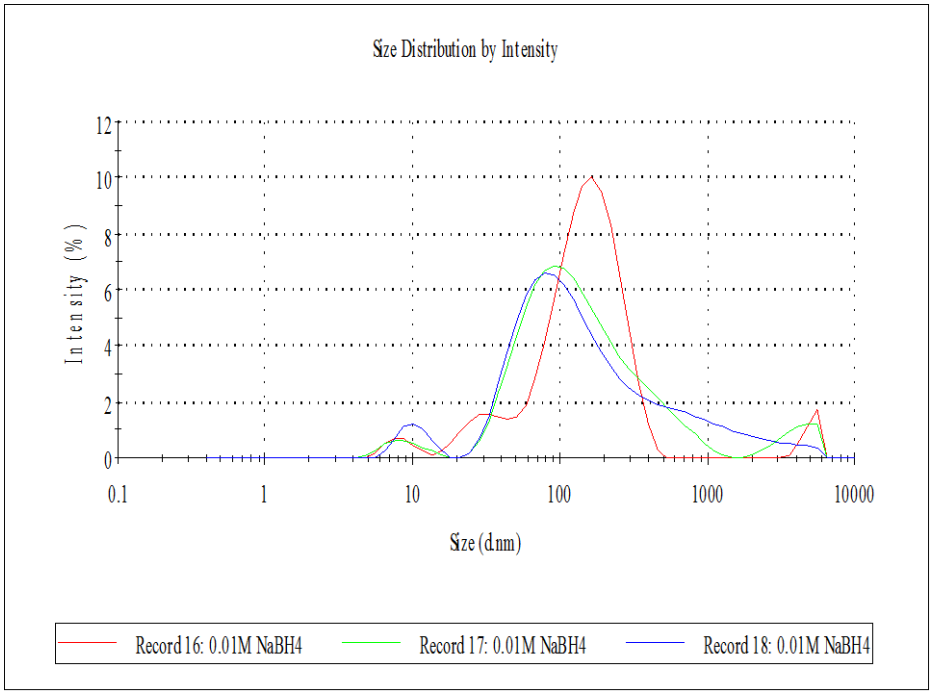

Figure 4.2. Size distribution by intensity of GNS reduced by $NaBH_4$ without PEG 1000.

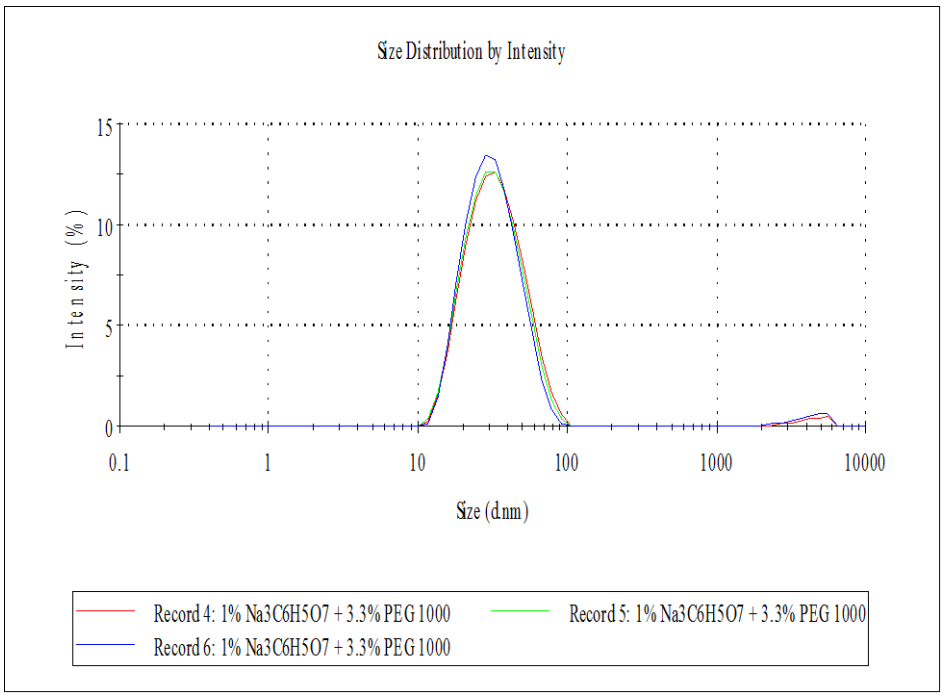

Figure 4.3. Size distribution by intensity of GNS reduced by $Na_3C_6H_5O_7$ with PEG 1000.

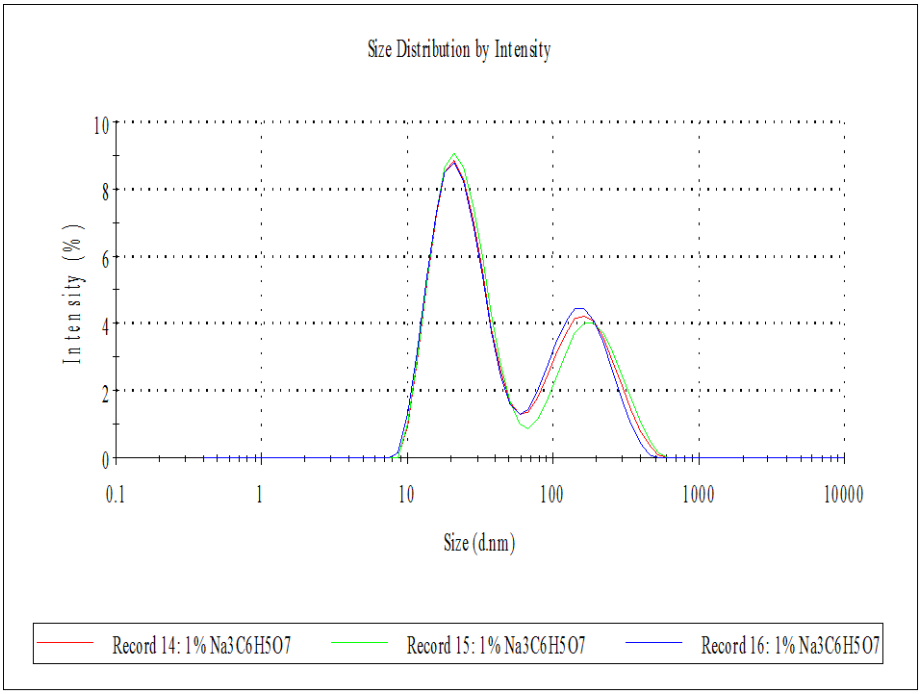

Figure 4.4. Size distribution by intensity of GNS reduced by $Na_3C_6H_5O_7$ without PEG 1000.

Table 4.1. Peak values and Z-average of the GNS samples.

No.	Sample	Peak(s) (nm)	Z-average (nm)
1	GNS reduced by $NaBH_4$ with PEG1000.	114.2	98.42 ± 0.13
2	GNS reduced by $NaBH_4$ without PEG1000.	84.5 372.9	90.72 ± 0.47
3	GNS reduced by $Na_3C_6H_5O_7$ with PEG1000.	35.83	29.57 ± 0.25
4	GNS reduced by $Na_3C_6H_5O_7$ without PEG1000	26.25 213.7	32.43 ± 0.46

The uniformity of the AuNPs plays important role in maintaining the stability of the gold nanoparticles. The uniformity of the gold nanoparticles shows the monodispersity of the GNS produced. The size distribution by intensity shows a peak when there are particles fall in the size range, and the amplitude of the peak reflects the amount of the particles present in the solution.

In this work, the results show obvious improvement on the stability and most importantly, the uniformity of the gold nanoparticles by adding PEG 1000 as the stabilizer. Figures 4.1 – 4.4 show the comparison of the particles size. With the PEG1000 as the stabilizer (Figures 4.1 and 4.3), the gold nanoparticles exhibit unimodal distribution compared to those without PEG1000 (Figures 4.2 and 4.4) which exhibited bimodal or multimodal distribution. We can clearly see that after the solution is stabilized by PEG 1000, it only shows one peak in the size distribution by intensity. This shows the AuNPs in the solution were uniform and thus monodispersed and stable.

The gold nanoparticles reduced by trisodium citrate has maintained their size for four weeks, while the gold nanoparticles reduced by sodium borohydride lasted less than 12 hours. The size distribution of the gold nanoparticles without PEG 1000 shows bimodal and polymodal distribution, which means the aggregation occurred. The PEG framework limited the growth of the gold nanoparticles, and make the nanoparticles grew uniformly (Chin et. al., 2012). The AuNPs were entrapped within the PEG framework, which decreased the chances of particles aggregation (Brandenberger et al., 2010), also

increased the stability (Serajuddin et al.). With this result, the GNS reduced by $Na_3C_6H_5O_7$ with PEG1000 is chosen to proceed with the LSPR characterization.

4.2.1.2 Localized Surface Plasmon Resonance

Figure 4.5 shows the UV-Vis Spectrum of GNS reduced by $Na_3C_6H_5O_7$ with PEG1000.

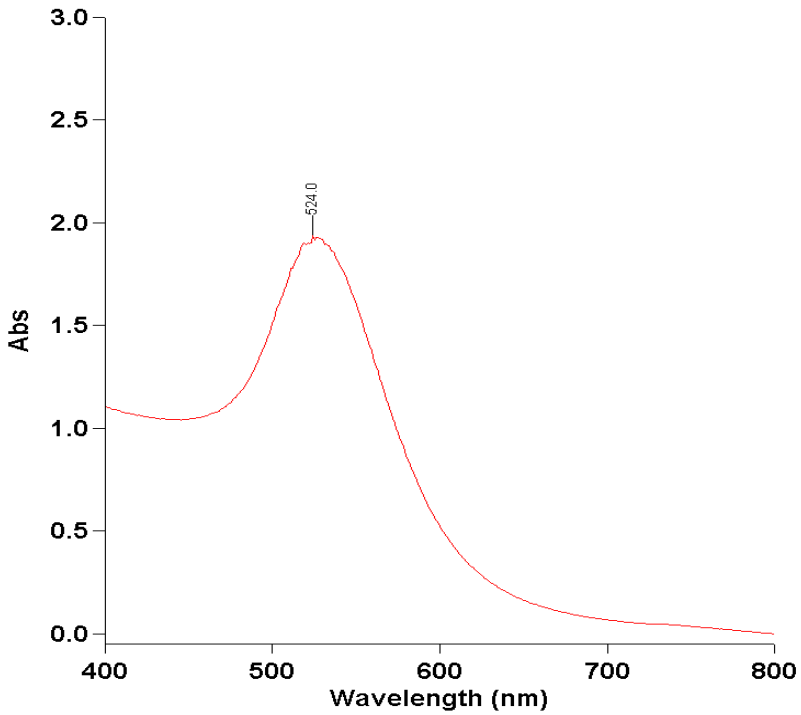

Figure 4.5. UV-Vis spectra of GNS which show λ_{max} at 524 nm

From the spectrum, the LSPR of the synthesized GNS with the particle size of 29.57 nm shows a strong absorbance band peaked at 524 nm, which falls in the visible region (390 nm - 700 nm). There is only 1 peak in the spectrum,

which is due to the spherical shape of the synthesized GNS is symmetry at all planar.

However, the intrinsic chromophores in human native tissues, and the haemoglobin in the blood and body tissues also absorbs the photon energy at visible wavelengths (Dickerson et al., 2008, Huang and El-Sayed, 2011). This interference and overlap of LSPR limited the possibilities of GNS to elevate the deep tumours to the therapeutic temperature (Afifi, 2013), but only to the shallow depth (Dickerson et al., 2008), or superficial type of cancers. For this reason, alternatives such as shifting the LSPR of the synthesized AuNPs out of the resonance of human tissues, for instance the near infra-red (NIR) spectra which range from 700 nm to 1000 nm, is able to avoid the overlapping of the LSPR of GNS to the human tissues. To achieve this, different morphological structure of the synthesized AuNPs should be obtained. Among which the rod shape AuNPs, or gold nanorod (GNR) was chosen in this work. The LSPR of GNR can be "tuned" to the NIR region, where the penetration of incident light may be achieved at depths exceeding 10 cm (Dickerson et al., 2008) through the tissues, and the penetration is optimal (Huang et al., 2008, Huang and El-Sayed, 2011) due to minimal attenuation.

4.2.1.3 Field Emission Scanning Electrode Microscopy

The synthesized GNS solutions were examined by FE-SEM to obtain the preliminary imaging results prior the more advance energy filtered transmission electron microscopy.

From the micrographs, the GNS reduced by $Na_3C_6H_5O_7$ without PEG 1000 (Figure 4.6) shows more uniform compared to the GNS reduced by $NaBH_4$ with PEG 1000 (Figure 4.7), which gold nanoparticles were not in spherical shape anymore. Also, the synthesized GNS show higher uniformity with and without PEG 1000 respectively (Figure 4.8 – Figure 4.9), which acts as the stabilizing agent in both $Na_3C_6H_5O_7$ and $NaBH_4$ reduced GNS. From here, we conclude that the GNS synthesized by $Na_3C_6H_5O_7$ reduction shows higher uniformity compared to $NaBH_4$, and the stabilizing agent further enhanced the uniformity and stability of the GNS produced.

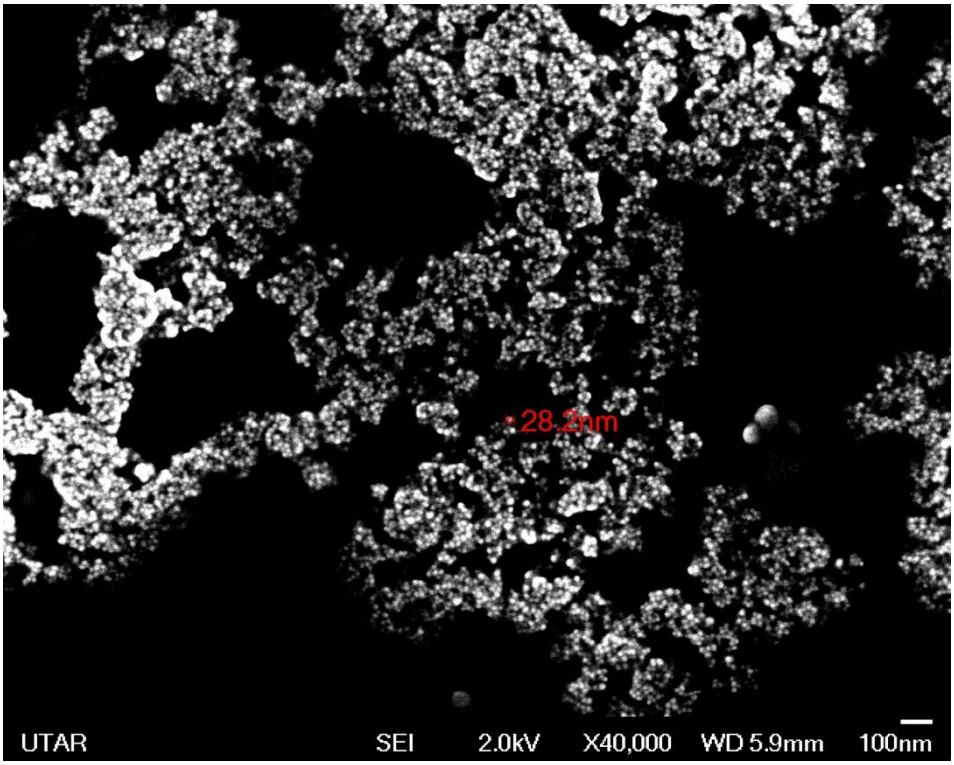

Figure 4.6. FE-SEM of GNS reduced by $Na_3C_6H_5O_7$ without PEG 1000.

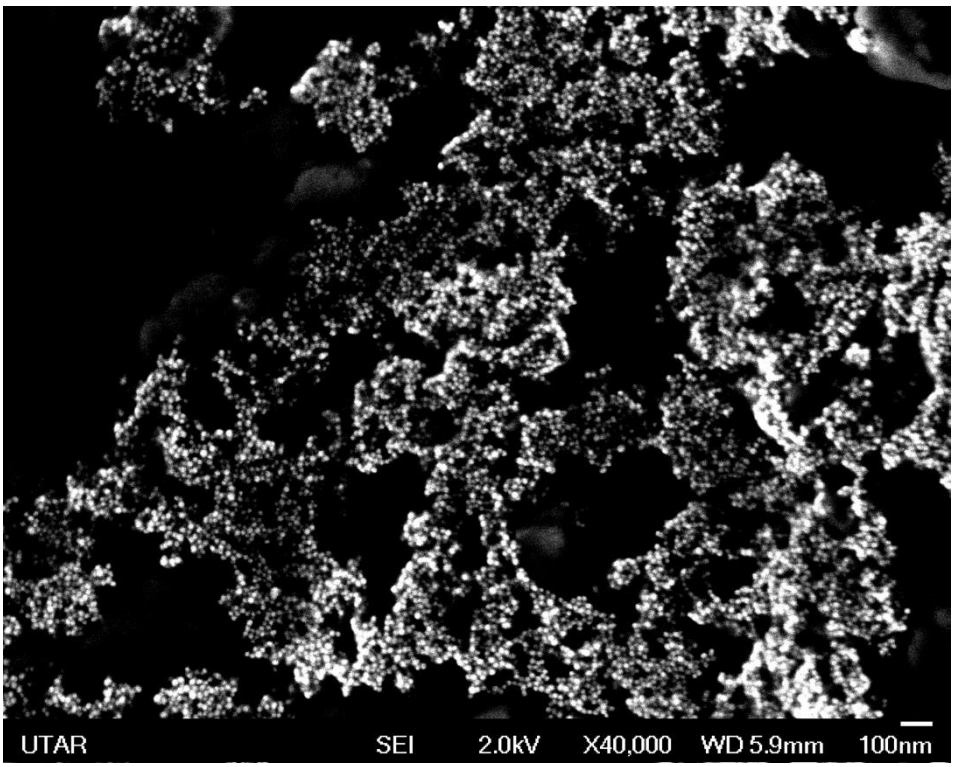

Figure 4.7. FE-SEM of GNS reduced by $NaBH_4$ with PEG 1000.

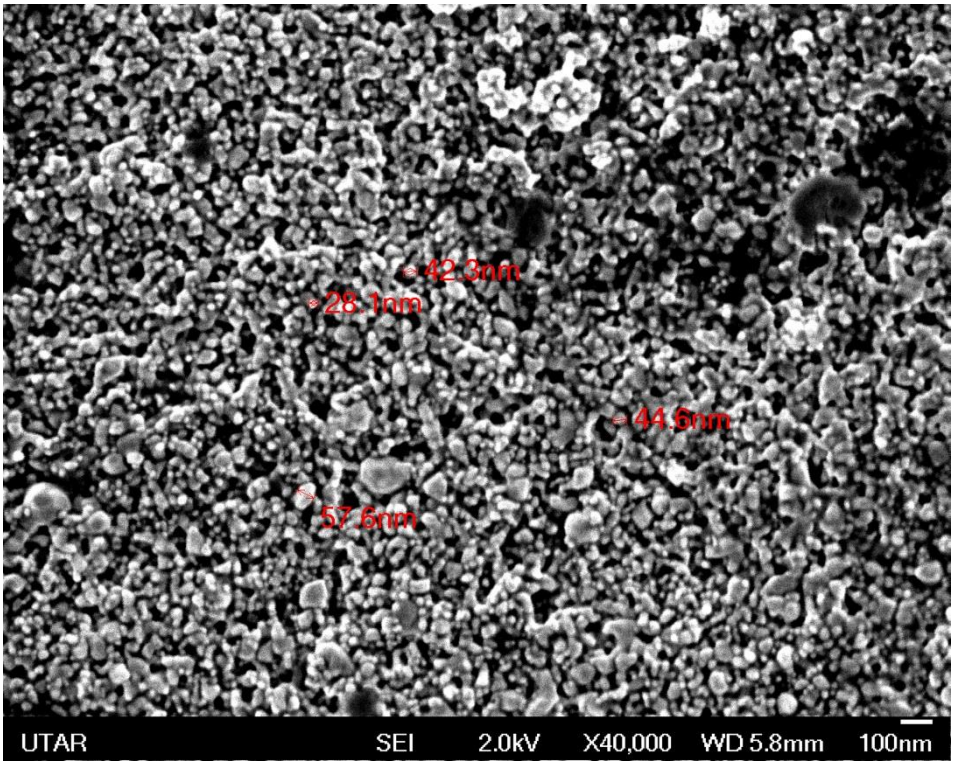

Figure 4.8. FE-SEM of GNS reduced by $NaBH_4$ without PEG 1000.

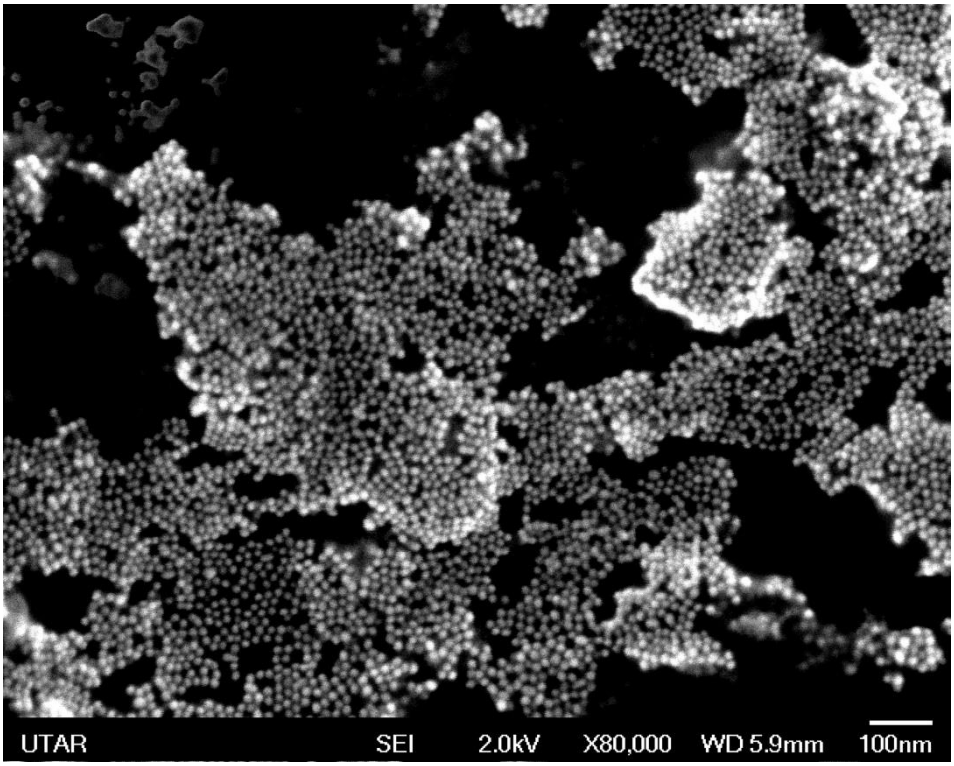

Figure 4.9. FE-SEM of GNS reduced by $Na_3C_6H_5O_7$ with PEG 1000.

4.2.1.4 Energy Filtered Transmission Electrode Microscopy

From the FE-SEM micrographs, the GNS by $Na_3C_6H_5O_7$ reduction proceeded to the EF-TEM for further characterization. From the EF-TEM microraphs, it shows that the synthesized GNS by $Na_3C_6H_5O_7$ reductions recorded the particle size at 30.58 nm ± 0.72 nm (Figure 4.10 – Figure 4.11), which is within the range of the targeted size range.

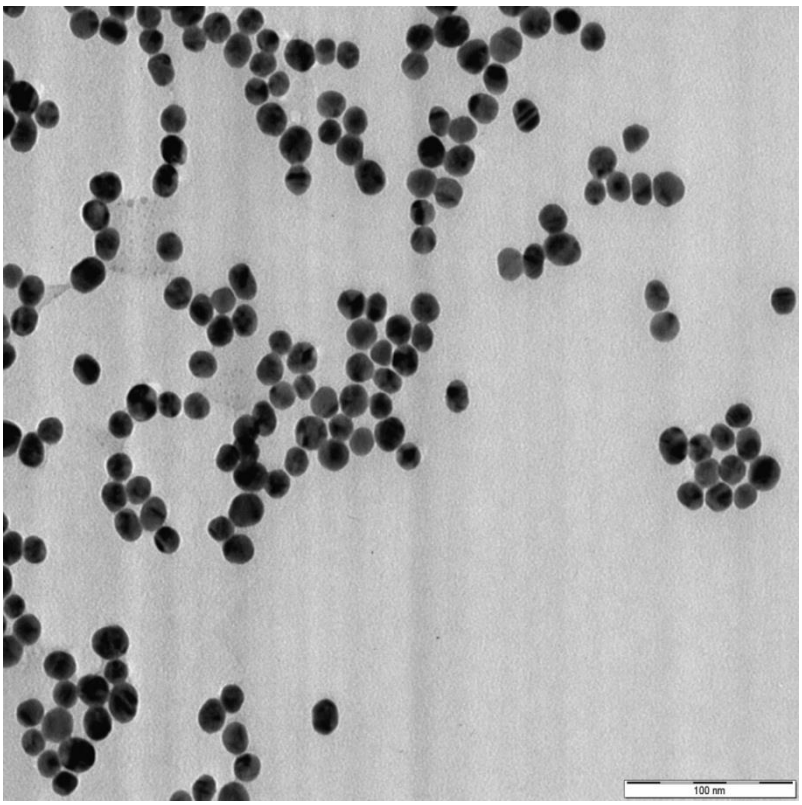

Figure 4.10. EF-TEM of GNS reduced by $Na_3C_6H_5O_7$ (Scale bar: 100 nm).

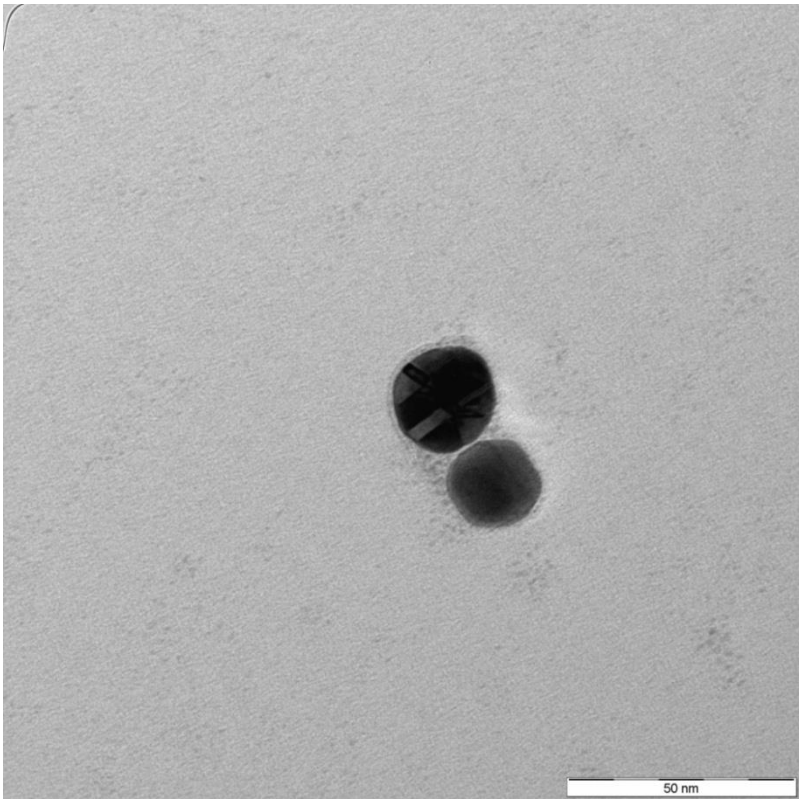

Figure 4.11. EF-TEM of GNS reduced by $Na_3C_6H_5O_7$ (Scale bar: 50 nm).

4.2.2 Characterization of the Gold Nanorod

Similar to GNS, the synthesized GNR were characterized using Zetasizer, FE-SEM, EF-TEM, and UV-Vis spectroscopy. The results are discussed in detail in the following sections.

The GNR remain their stability due to the present of the CTAB surfactant which surrounded the GNR particles. The CTAB prevents the GNR particles from interacting each other, as well as keeping the GNR intact. Hence, there is no stability agent added to the GNR solution.

4.2.2.1 Localized Surface Plasmon Resonance

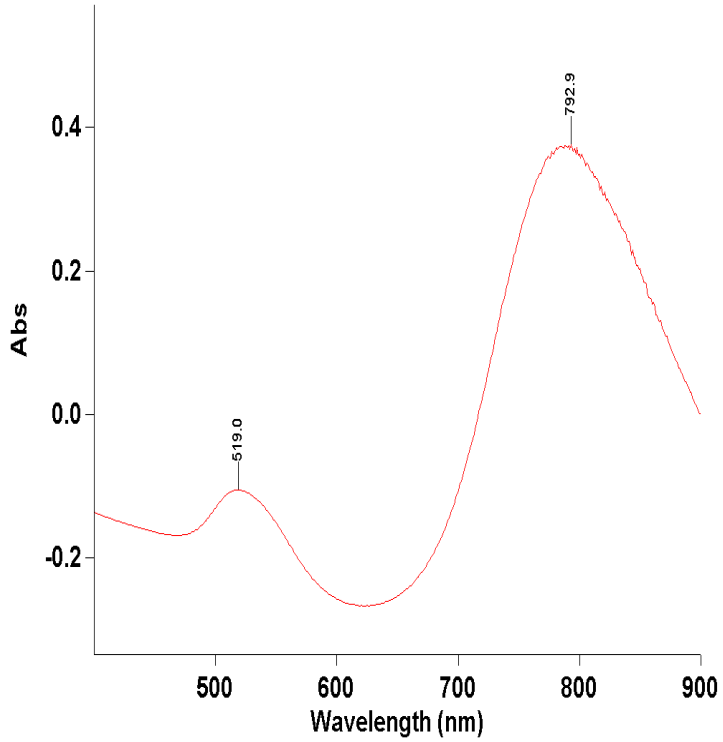

Figure 4.12. UV-Vis spectra of GNR which shows 2 peaks at 519 nm (Transverse) and 793 nm (Longitudinal).

4.2.2.2 Field Emission Scanning Electrode Microscopy

From the UV-Vis spectrum, the LSPR of the synthesized GNR showed two strong absorbance bands, which the first absorbance band peaked at 519 nm that falls in the visible region (390 nm - 700 nm), and the second absorbance band,

which exhibits higher absorbance compared to the first peak, peaked at 793nm that is in the near infra-red (NIR) region (700 nm – 1100 nm) (Figure 4.12).

The first peak in the UV-Vis spectrum represents the GNR's LSPR of the transverse plane (shorter plane), while the second peak represents the GNR's LSPR of the longitudinal plane (longer plane). In other words, the LSPR around 519 nm corresponds to the oscillation of the electrons perpendicular to the major (long) rod axis, and is referred to as the transverse plasmon absorption. This is because the shape and diameter of the transverse plane of the GNR is similar to a GNS. As for the second peak, which represents the longitudinal plane of the GNR is showing the LSPR at NIR region (793 nm). This LSPR is being produced by the oscillation of the electrons in parallel to the major (long) rod axis, and is known as the longitudinal surface plasmon absorption. This finding is very crucial for this work. As discussed in the earlier section, the LSPR peak in the NIR wavelength of GNR enables the incident light or the laser source to penetrate through the tissues due to minimal energy absorption at this spectrum. Herein, the longitudinal LSPR is closely depends on the aspect ratio of the GNR, which is the ratio of length to width of the GNR. The GNR synthesized in this study has reported an average aspect ratio of 2.98 ± 0.16, which produces the longitudinal LSPR at 793 nm. With higher aspect ratio, LSPR will be red-shifted towards longer wavelength up to 1500 nm. The aspect ratio is discussed further in the following section.

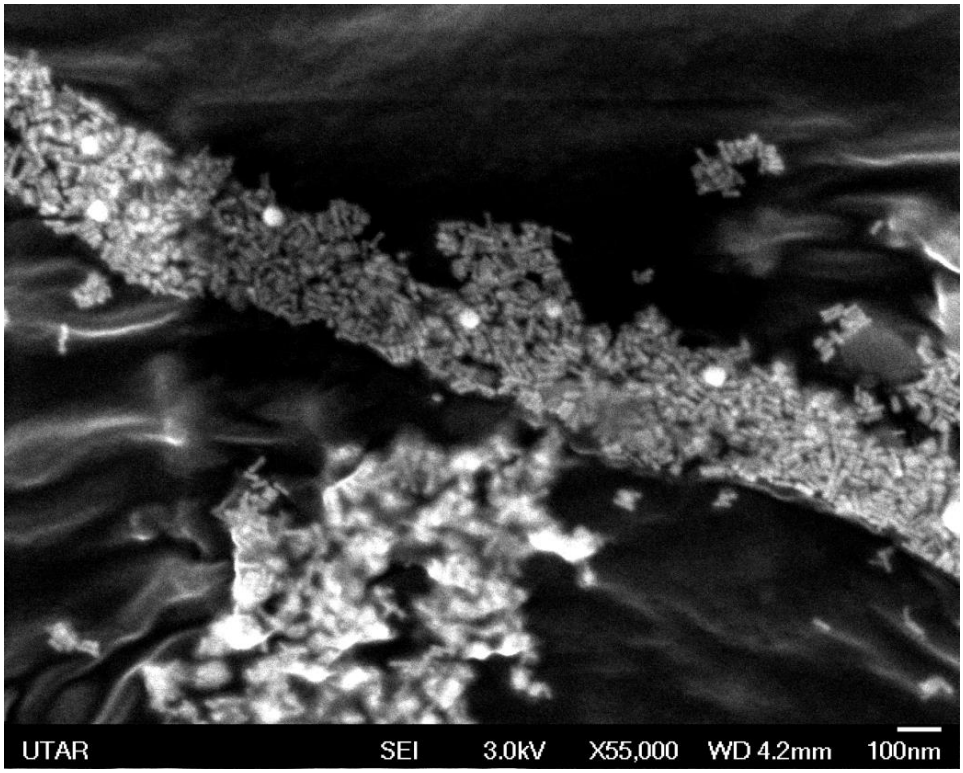

Figure 4.13. FE-SEM of GNR (Scale bar: 100 nm).

From Figure 4.14, the GNR produced by the seed-mediated growth methods showed the preliminary results of the cylindrical/rod shape of the GNR. This result enables us to proceed to the EF-TEM for more advance imaging.

4.2.2.3 Energy Filtered Transmission Electrode Microscopy

From the result of the FE-SEM micrographs, we have proceeded the GNR for the EF-TEM for further characterization.

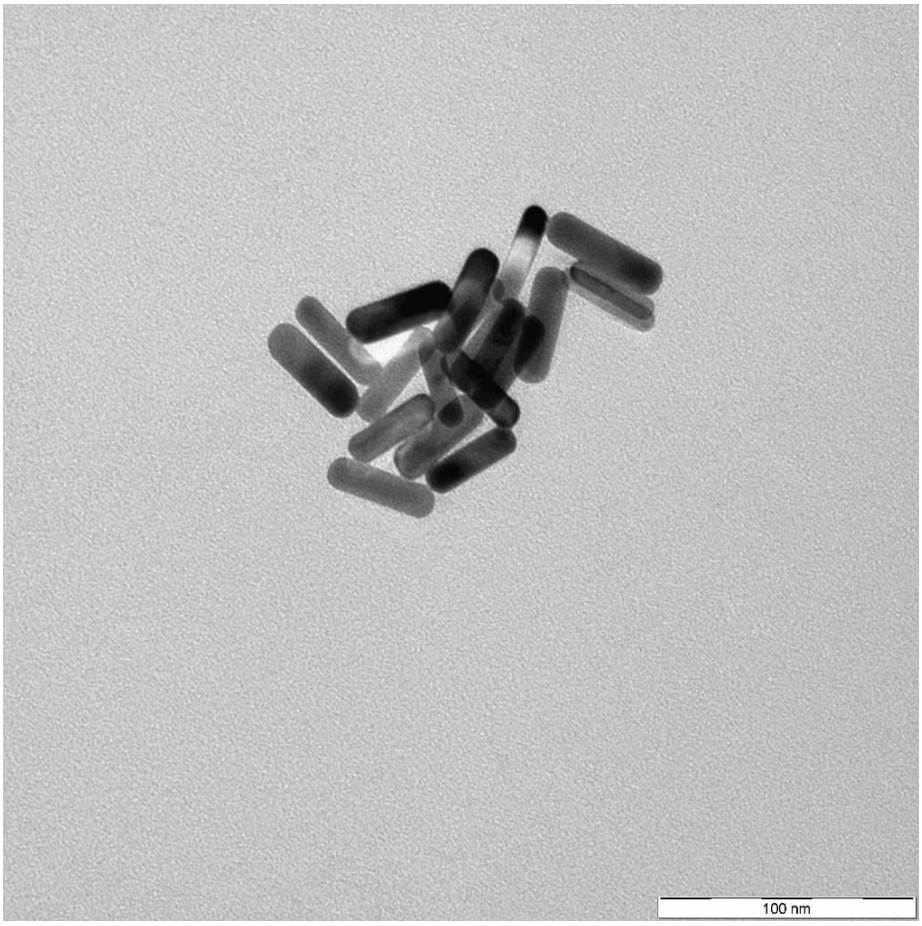

Figure 4.14. EF-TEM of GNR (Scale bar: 100 nm).

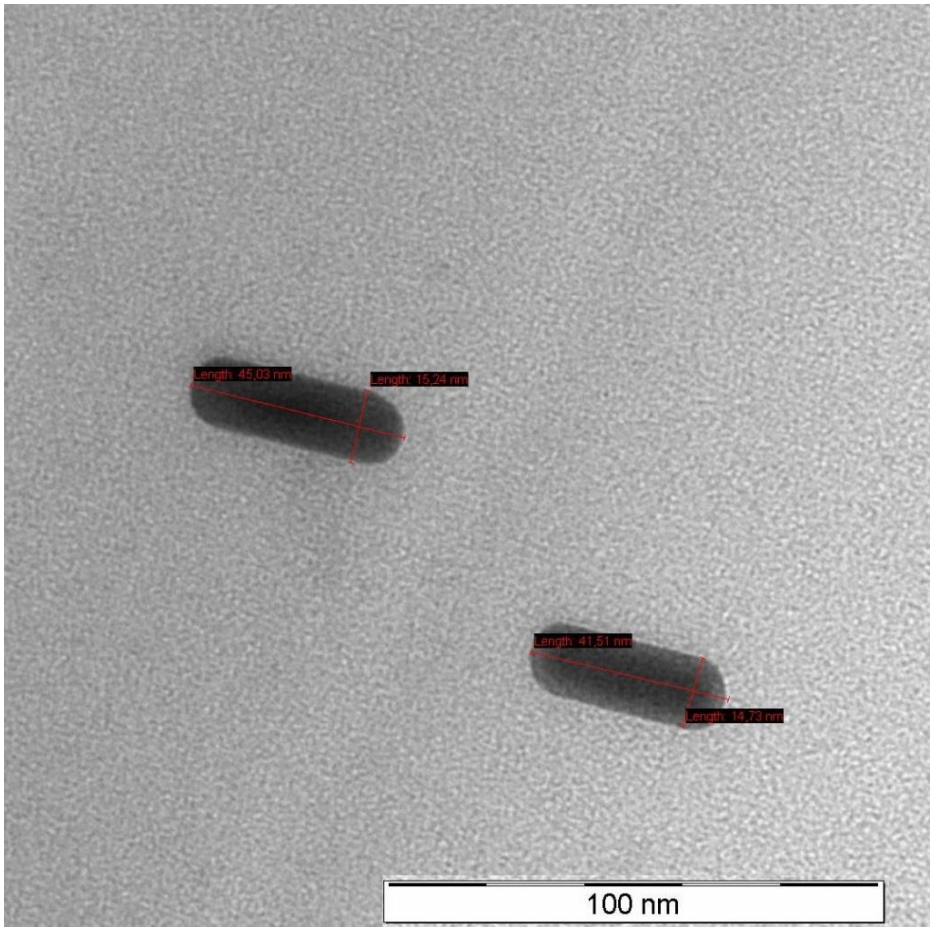

Figure 4.15. EF-TEM of GNR with measurements labels (Scale bar: 100 nm).

From Figure 4.15, it shows that the synthesized GNR have the size of 43.27 nm ± 1.76 nm, which is within the range of the targeted size range. As discussed in the previous section, the aspect ratio is being calculated by dividing the long axis (length) by the short axis (width) of the GNR. In this work, in order to produce the longitudinal length <50nm, but LSPR >700nm, the targeted aspect ratio of the synthesized GNR is '3'. The GNR synthesized in this study has reported an average aspect ratio of 2.98 ± 0.16. However, high aspect ratio is not necessary in the cancer treatment because with higher aspect ratio, the

size of the GNR is increased. Larger GNR exhibits lower EPR effect, which causing the GNR to lose their passive targeting ability to the cancer cells.

CHAPTER FIVE

CONCLUSION AND RECOMMENDATION

5.1 Conclusion

The primary objective of this research work is to synthesize the AuNPs in spherical and rod shape, together with the characterization of the AuNPs. The methods used and the results published from this work can be applied to future work towards understanding and facilitating the integration of the non-invasive cancer treatment in the market. In this work, the preparation methods of the GNS and GNR have been described. Two methods were reported in the GNS synthesis methodology, namely citrate-reduction and sodium borohydride reduction. From the results, the GNS synthesized by $Na_3C_6H_5O_7$ reduction shows higher uniformity compared to $NaBH_4$, and the stabilizing agent further enhanced the uniformity and stability of the GNS produced. The GNS recorded the size at 30.58 nm ± 0.72 nm, within the targeted size range of 20 nm to 50 nm. The GNS also recorded a single peak at 524nm which falls under visible wavelengths.

On the other hand, GNR is synthesized by the seed-mediated growth method. The GNR synthesized recorded an average aspect ratio of 2.98 ± 0.16, which also fall within the targeted size range of 20 nm to 50 nm. The LSPR of the GNR recorded at 793 nm for the longitudinal plane, and 519 nm for the

transverse plane. The examination of FE-SEM and EF-TEM also enhanced the characterization of the AuNPs by providing the physical image of the produced AuNPs. Generally, the synthesize work of the GNS and GNR is achieved.

5.2 Recommendation and Future Works

5.2.1 Plasmonic Photothermal Therapy Efficacy Test

As discussed in the literature review, the application of PPTT used the photon energy of the incident light source, which is selectively administered into the targeted body part, and being converted into heat to provide a minimally-invasive oncological treatment by inducing the cellular hyperthermia. With the synthesized GNR which has the longitudinal plane LSPR that is in the NIR wavelength range, it can solve the interference and overlapping of the LSPR with water and the intrinsic chromophores, which has limited the Gold nanoparticles, particularly the GNS in PPTT, as well as increase the efficacy.

5.2.2 *In-Vivo* Test on Experimental Rat

With the possibility of the enhanced PPTT, the *in-vivo* test on the experimental rat is one of the future work that enabled the study of the efficacy of the synthesized GNR, as well as the systemic toxicity level. The study can be done by injecting the GNR solution into the experimental rat, which can be

divided into study group and control group. The study group will be induced with the tumour cell, while the control group will be the healthy group. Both of the group will be irradiated with the excitation incident light that is matched to the LSPR of the GNR. This study will provide the efficacy of the GNR, as well as the adverse effect test and systemic toxicity test.

5.2.3 Clearance Methods of Gold Nanoparticles

As the AuNPs possessed the EPR effect, it has enabled the AuNPs to accumulate around the tumour tissues, but the particles will also be accumulated at the lymph system and the hepatic system as they are the "clearance system" of our body. Although there is no report of adverse effect on gold nanoparticles, it is essential to study the clearance of the gold nanoparticles that will be remained in the human body. Methods such as surface modification/coating of the gold nanoparticles with different materials to assist in the clearance of the AuNPs is one of the major works to work on.

REFERENCE LIST

Afifi, M. M., El Sheikh, S. M., Abdelsalam, M.M., Ramadan, H., Omar, T. A., El Tantawi, M., Abdelrazek, K., Mohamed, M., 2013. Therapeutic efficacy of plasmonic photothermal nanoparticles in hamster buccal pouch carcinoma. *Oral surgery, oral medicine, oral pathology and oral radiology*.

Aillon, K. L., Xie, Y., El-Gendy, N., Berkland, C. J., Forrest, M. L., 2009. Effects of nanomaterial physicochemical properties on in vivo toxicity. *Advanced Drug Delivery Reviews, 61*(6), 457 - 466.

Akbarzadeh, A., Zare, D., Farhangi, A., Mehrabi, M. R., Norouzian, D., Tangestaninejad, S., Moghadam, M., Bararpour, N., 2009. Synthesis and characterization of gold nanoparticles by tryptophane. *American Journal of Applied Sciences, 6*(4), 691.

Arsianti, M., Lim, M., Lou, S. N., Goon, I. Y., Marquis, C. P., Amal, R., 2011. Bi-functional gold-coated magnetite composites with improved biocompatibility. *Journal of Colloid and Interface Science, 354*(2), 536 - 545.

Baban, D. F., & Seymour, L. W., 1998. Control of tumour vascular permeability. *Advanced Drug Delivery Reviews, 34*(1), 109 - 119.

Baik, H. J., Hong, S., Park, S., 2011. Surface plasmon modes of gold nanospheres, nanorods, and nanoplates in an organic solvent: Phase-transfer from aqueous to organic media. *Journal of Colloid and Interface Science, 358*(2), 317 - 322.

Bernard, V., Mornstein, V., Jaroš, J., Sedláčková, M., & Škorpíková, J., 2014. Combined effect of silver nanoparticles and therapeutical ultrasound on ovarian carcinoma cells A2780. *Journal of Applied Biomedicine, 12*(3), 137 - 145.

Bhana, S., O'Connor, R., Johnson, J., Ziebarth, J. D., Henderson, L., & Huang, X., 2016. Photosensitizer-loaded gold nanorods for near infrared photodynamic and photothermal cancer therapy. *Journal of Colloid and Interface Science, 469*, 8 - 16.

Bhattacharyya, S., Kudgus, R. A., Bhattacharya, R., & Mukherjee, P., 2011. Inorganic Nanoparticles in Cancer Therapy. *Pharmaceutical Research, 28*(2), 237 - 259.

Brandenberger, C., Mühlfeld, C., Ali, Z., Lenz, A.-G., Schmid, O., Parak, W. J., Rothen-Rutishauser, B., 2010. Quantitative evaluation of cellular uptake and trafficking of plain and polyethylene glycol-coated gold nanoparticles. *Small (Weinheim an der Bergstrasse, Germany), 6*(15), 1669-1678. doi: 10.1002/smll.201000528

Chen, X., & Schluesener, H. J., 2008. Nanosilver: A nanoproduct in medical application. *Toxicology Letters, 176*(1), 1 - 12.

Chin, G. F., Misran, M., Tang, P. Y., & Lee, P. F., 2013. *Synthesizing Gold Nanoparticles in Spherical and Rod Shapes for Targeting Cancer Treatment*. Paper presented at the The 15th International Conference on Biomedical Engineering.

Chin, G. F., Misran, M., Tang, P. Y., Lee, P. F., 2012. *Signal analysis with Zetasizer on the effect of Poly (Ethylene Glycol)(PEG) to stabilize and unify colloidal gold nanoparticles.* Paper presented at the Biomedical Engineering (ICoBE), 2012 International Conference on.

Cho, W.-S., Cho, M. Jeong, J., Choi, M., Cho, H. -Y., Han, B. S., Kim, S. H., Kim, H. O., Lim, Y. T., Chung, B. H., 2009. Acute toxicity and pharmacokinetics of 13 nm-sized PEG-coated gold nanoparticles. *Toxicology and applied pharmacology, 236*(1), 16-24.

Daniel, M. C., & Astruc, D., 2004. Gold nanoparticles: assembly, supramolecular chemistry, quantum-size-related properties, and applications toward biology, catalysis, and nanotechnology. *Chem. Rev., 104*, 293 - 346.

DeMesster, T. R., & Barlow, A. P., 1988. Surgery and current management for cancer of the esophagus and cardia. *Current Problems in Cancer, 12*(5), 243 - 328.

Dickerson, E. B., Dreaden, E. C., Huang, X., El-Sayed, I. H., Chu, H., Pushpanketh, S., El-Sayed, M. A., 2008. Gold nanorod assisted near-infrared plasmonic photothermal therapy (PPTT) of squamous cell carcinoma in mice. *Cancer letters, 269*(1), 57 - 66.

El-Sayed, I. H., Huang, X., El-Sayed, M. A., 2005. Surface plasmon resonance scattering and absorption of anti-EGFR antibody conjugated gold nanoparticles in cancer diagnostics: applications in oral cancer. *Nano letters, 5*(5), 829 - 834.

Elechiguerra, J. L., Burt, J. L., Morones, J. R., Camacho-Bragado, A., Gao, X., Lara, H. H., & Yacaman, M. J., 2005. Interaction of silver nanoparticles with HIV-1. *J Nanobiotechnology, 3*(6). doi: 10.1186/1477-3155-3-6

Esther H. Chang, J. B. H., Michael A.W. Eaton, Patrick M. Boisseau, Admire Dube, Rose Hayeshi, Hulda Swai, Dong Soo Lee., 2015. Nanomedicine: Past, present and future – A global perspective. *Biochemical and Biophysical Research Communications, 468*(3), 511 - 517.

Etheridge, M. L., Campbell, S. A., Erdman, A. G., Haynes, C. L., Wolf, S. M., McCullough, J., 2012. The big picture on nanomedicine: the state of investigational and approved nanomedicine products. *Nanomedicine: Nanotechnology, Biology, and Medicine*.

F. K. Alanazi, A. A. R., I. A. Alsarra., 2010. Biopharmaceutical applications of nanogold. *Saudi Pharmaceutical Journal King, 18*, 179 - 193.

Faedmaleki, F., Shirazi, F. H., Salarian, A.-A., Ashtiani, H. A., & Rastegara, H., 2014. Toxicity Effect of Silver Nanoparticles on Mice Liver Primary Cell Culture and HepG2 Cell Line. *Iranian Journal of Pharmaceutical Research, 13*(1), 235 - 242.

Flower, G. L., Latha, S. V., & Rao, K. V., 2016. Novel characterization of nanosilver fluid through ultrasonic studies supported by UV–Vis spectroscopy, DLS and TEM studies. *Journal of Molecular Liquids, 221*, 333 - 338.

Furr, J. R., Russell, A. D., Turner, T. D., & Andrews, A., 1994. Antibacterial activity of Actisorb Plus, Actisorb and silver nitrate. *Journal of Hospital Infection, 27*(3), 201 - 208.

Galdiero, S., Falanga, A., Vitiello, M., Cantisani, M., Marra, V., & Galdiero, M., 2011. Silver Nanoparticles as Potential Antiviral Agents *Molecules, 16*, 8894 - 8918. doi: 10.3390/molecules16108894

Ghosh, P., Han, G., De, M., Kim, C. K., & Rotello, V. M., 2008. Gold nanoparticles in delivery applications. *Advanced Drug Delivery Reviews 60*(1), 307-1315.

Gormley, A. J., Greish, K., Ray, A., Robinson, A., Gustafson, J. A., & Ghandehari, H., 2011. Gold nanorod mediated plasmonic photothermal therapy: A tool to enhance macromolecular delivery. *International Journal of Pharmaceutics 415* 315 - 318.

Granmayeh Rad, A., Abbasi, H., & Afzali, M. H., 2011. Gold Nanoparticles: Synthesising, Characterizing and Reviewing Novel Application in Recent Years. *Physics Procedia, 22*, 203-208.

Guo, J., O'Driscoll, C. M., Holmes, J. D., & Rahme, K., 2016. Bioconjugated gold nanoparticles enhance cellular uptake: A proof of concept study for siRNA delivery in prostate cancer cells. *International Journal of Pharmaceutics, 509*(1 - 2), 16 - 27.

Hamouda, I. M., 2012. Current perspectives of nanoparticles in medical and dental biomaterials. *Journal of Biomedical Research, 26*(3), 143 - 151.

Huaizhi, Z., & Yuantao, N., 2000. *China's Ancient Gold Drugs*. Paper presented at the Symposium on Gold and Silver Catalysis, University of Limerick, Ireland,.

Huang, X., & El-Sayed, M. A., 2011. Plasmonic photo-thermal therapy (PPTT). *Alexandria Journal of Medicine, 47*(1), 1 - 9.

Huang, X., Jain, P. K., El-Sayed, I. H., & El-Sayed, M. A., 2008. Plasmonic photothermal therapy (PPTT) using gold nanoparticles. *Lasers in medical science, 23*(3), 217 - 228.

Inaga, S., Osatake, H., & Tanaka, K., 1991. SEM Images of DNA Double Helix and Nucleosomes Observed by Ultrahigh-Resolution Scanning Electron Microscopy. *Journal of Electron Microscopy, 10*(3), 181 - 186.

Jain, P. K., El-Sayed, M. A., 2010. Plasmonic coupling in noble metal nanostructures. *Chemical Physics Letters, 487*(4), 153 - 164.

Jose, M., Dhas, S. A. M. B., Daisy, A. D., & Das, S. J., 2016. Synthesis and characterization of nano spheres decorated silver bromide nanorods using a two step chemical reduction route. *Optik - International Journal for Light and Electron Optics, 127*(19), 8019 - 8023.

Jr, F. R., 2005. What is nanomedicine? *Nanomedicine: Nanotechnology, Biology, and Medicine, 1*, 2 - 9.

Karonidis, A., Delikonstantinou, I., & Tsoutsos, D., 2011. Use of Actisorb* dressings over a skin-grafted infected wound. *Burns, 37*(2), 360 - 361.

Kawasaki, E. S., & Player, T. A., 2005. Nanotechnology, nanomedicine, and the development of new, effective therapies for cancer. *Nanomedicine: Nanotechnology, Biology, and Medicine 1*, 101- 109.

Kihm, K. D., Cheon, S., Park, J. S., Kim, H. J., Lee, J. S., Kim, I. T., & Yi, H. J., 2012. Surface plasmon resonance (SPR) reflectance imaging: Far-field recognition of near-field phenomena. *Optics and Lasers in Engineering, 50*(1), 64 - 73.

Kolodgie, F. D., Narula, J., Yuan, C., Burke, A. P., Finn, A. V., & Virmani, R., 2007. Elimination of Neoangiogenesis for Plaque StabilizationIs There a Role for Local Drug Therapy? *Journal of the American College of Cardiology, 49*(21), 2093 - 2101.

Kumar, R., Shukla, S. K., Pandey, M., Pandey, A., Pathak, A., & Dikshit, A., 2016. Synthesis and antimicrobial effects of colloidal gold nanoparticles against prevalent waterborne bacterial pathogens. *Cogent Chemistry 2*, 1192522.

Lara, H. H., Garza-Treviño, E. N., Ixtepan-Turrent, L., & Singh, D. K., 2011. Silver nanoparticles are broad-spectrum bactericidal and virucidal compounds. *J Nanobiotechnology*, *9*(30). doi: 10.1186/1477-3155-9-30

Liu, K.-G., Abbasi, A. R., Azadbakht, A., Hu, M.-L., & Morsali, A., 2017. Deposition of silver nanoparticles on polyester fiber under ultrasound irradiations. *Ultrasonics Sonochemistry, 34*, 13 - 18.

Lombardi, L., Morelli, F., Cinieri, S., Santini, D., Silvestris, N., Fazio, N., . . . Maiello, E., 2010. Adjuvant colon cancer chemotherapy: where we are and where we'll go. *Cancer Treatment Reviews, 36*(3), 34 - 41.

Miller, A. C., Rashid, R. M., Falzon, L., Elamin, E. M., & Zehtabchi, S., 2012. Silver sulfadiazine for the treatment of partial-thickness burns and venous stasis ulcers *Journal of the American Academy of Dermatology, 66*(5), 159 - 165.

Mukherjee, P., Bhattacharya, R., Bone, N., Lee, Y. K., Patra, C. R., Wang, S., Mukhopadhyay, D., 2013. Correction: Potential therapeutic application of gold nanoparticles in B-chronic lymphocytic leukemia (BCLL): enhancing apoptosis. *J Nanobiotechnology., 5*(4). doi: 10.1186/1477-3155-11-23

Murphy, C. J., Thompson, L. B., Chernak, D. J., Yang, J. A., Sivapalan, S. T., Boulos, S. P., Sisco, P. N., 2011. Gold nanorod crystal growth: from seed-mediated synthesis to nanoscale sculpting. *Current Opinion in Colloid & Interface Science, 16*(2), 128 - 134.

Naahidi, S., Jafari, M., Edalat, F., Raymond, K., Khademhosseini, A., & Chen, P., 2012. Biocompatibility of engineered nanoparticles for drug delivery. *Journal of controlled release*.

Narang, A., & Varia, S., 2011. Role of tumor vascular architecture in drug delivery. *Advanced Drug Delivery Reviews 63*(8), 640 - 658.

Palaniappan, P., Sathishkumar, G., & Sankar, R., 2015. Fabrication of nano-silver particles using Cymodocea serrulata and its cytotoxicity effect against human lung cancer A549 cells line. *Spectrochimica Acta Part A: Molecular and Biomolecular Spectroscopy, 138*, 885 - 890.

Papasani, M. R., Wang, G., Hill, R. A., 2012. Gold nanoparticles: the importance of physiological principles to devise strategies for targeted drug delivery. *Nanomedicine: Nanotechnology, Biology and Medicine, 8*(6), 804-814.

Rai, M., Ingle, A. P., Gupta, I., & Brandelli, A., 2015. Noble Metal Nanoparticles: Synthesis and Optical Properties. *International Journal of Pharmaceutics, 496*(2), 159 - 172.

Ribatti, D., Nico, B., Crivellato, E., & Vacca, A., 2007. The structure of the vascular network of tumors. *Cancer letters, 248*(1), 18 - 23.

Richards, D. G., McMillin, D. L., Mein, E. A., & Nelson, C. D., 2002. Gold And Its Relationship To Neurological/Glandular Conditions. *International Journal of Neuroscience, 122,* 31 - 53.

Sandri, G., Bonferoni, M. C., D'Autilia, F., Rossi, S., Ferrari, F., Grisoli, P., Caramella, C., 2013. Wound dressings based on silver sulfadiazine solid lipid nanoparticles for tissue repairing. *European Journal of Pharmaceutics and Biopharmaceutics, 84*(1), 84 - 90.

Serajuddin, A. T. M., Mufson, D., Bernstein, D. F., Sheen, P.-C., & Augustine, M. A., 1988. Effect of Vehicle Amphiphilicity on the Dissolution and Bioavailability of a Poorly Water-Soluble Drug from Solid Dispersions. *Journal of Pharmaceutical Sciences, 77*(5), 414-417. doi: 10.1002/jps.2600770512

Sergeev, B. M., Kasaikin, V. A., Litmanovich, E. A., Sergeev, G. B., & Prusov, A. N., 1999. Cryochemical synthesis and properties of silver nanoparticle dispersions stabilised by poly(2-dimethylaminoethyl methacrylate). *Mendeleev Communications, 9*(4), 130 - 131.

Sheehy, K., Casey, A., Murphy, A., & Chambers, G., 2014. Antimicrobial properties of nano-silver: A cautionary approach to ionic interference. *Journal of Colloid and Interface Science, 443,* 56 - 64.

Tao, L., Guohua, M., & Tongjiang, P., 2015. Mechanism of Preparing Spherical Nano-sized Silver Particles via o-Phenylenediamine Reduction Process in Water-NMPD Mixed Solution System. *Rare Metal Materials and Engineering, 44*(5), 1071 - 1074.

Vaidyanathan, R., Kalishwaralal, K., Gopalram, S., & Gurunathan, S., 2009. Nanosilver—The burgeoning therapeutic molecule and its green synthesis. *Biotechnology Advances, 27,* 924 - 937.

Vlăsceanu, G. M., Marin, Ş., Ţiplea, R. E., Bucur, I. R., Lemnaru, M., Marin, M. M., . . . Andronescu, E., 2016. Chapter 2 – Silver nanoparticles in cancer therapy. *Nanobiomaterials in Cancer Therapy*, *7*, 29 - 56.

Wang, Z. L., 2000. Transmission Electron Microscopy of Shape-Controlled Nanocrystals and Their Assemblies. *The Journal of Physical Chemistry B, 104*, 1153 - 1175.

Zhao, L., Kim, T.-H., Kim, H.-W., Ahn, J.-C., & Kim, S. Y., 2016. Enhanced cellular uptake and phototoxicity of Verteporfin-conjugated gold nanoparticles as theranostic nanocarriers for targeted photodynamic therapy and imaging of cancers. *Materials Science and Engineering: C, 67*, 611 - 622.

Zhou, J., Tang, D., Hou, L., Cui, Y., Chen, H., & Chen, G., 2012. Nanoplatinum-enclosed gold nanocores as catalytically promoted nanolabels for sensitive electrochemical immunoassay. *Analytica Chimica Acta, 751*(2), 52 - 58.